Protonation and Alkylation of the Thiolato Donors in [Fe(CO)("N_HS_4")]: Effects on the Structural, Electronic, and Redox Properties of Metal–Sulfur Complexes**

Dieter Sellmann,* Thomas Becker, and Falk Knoch

Dedicated to Professor Rudolf Taube on the occasion of his 65th birthday

Abstract: The effects of protonation and alkylation at the sulfur donors in metal–sulfur complexes have been investigated by taking the specific example of [Fe(CO)("N_HS_4")] (**1**). The 18 valence electron (VE) complex **1** consists of a low-spin Fe^{II} center and the dithioether thiolato amine ligand "N_HS_4"$^{2-}$ (= 2,2′-bis(2-mercaptophenylthio)diethylamine(2 −)). Complex **1** can be reversibly protonated at the two thiolato donors; this results in an increase in ν(CO) of 35 cm^{-1} after the first protonation and 45 cm^{-1} after the second. Alkylation of **1** with one or two equivalents of the oxonium salts R_3OBF_4 (R = Me, Et) yields [Fe(CO)("N_HS_4"-R)]BF_4 (R = Me: **4**, Et: **5**), [Fe(CO)("N_HS_4"-R_2)]$(BF_4)_2$ (R = Me: **6**, Et: **7**), and the methyl ethyl derivative [Fe(CO)("N_HS_4"-Me-Et)]$(BF_4)_2$ (**8**). An increase in ν(CO) of 31–32 cm^{-1} is observed for each successive alkylation. Due to the C_1 symmetry of **1**, complexes **4**, **5**, and **8** are formed as 1:1 mixtures of two diastereomers, whereas **6** and **7** are present as only one stereoisomer. Acidic hydrolysis of **4**, **6**, and **7** liberates the corresponding ligands ["$N_{H2}S_4$"-R_n]$(BF_4)_n$ (**9**–**11**; n = 1,2), which were isolated as the ammonium tetrafluoroborate salts. The molecular structure of **8a** has been elucidated by X-ray structure analysis. This shows that the Fe–N and Fe–S bonds in the [$FeNS_4$] core do not change after alkylation of the thiolato donors despite the $\Delta\nu$(CO) of ca. 60 cm^{-1} between **1** and **8**, which indicates a distinct decrease in electron density at the Fe center. This decrease can be rationalized by increased π-acceptor character of the sulfur donors upon protonation or alkylation. The change in electron density at the [Fe("NS_4")] core is further corroborated by cyclic voltammetry. For each successive protonation or alkylation of **1**, the redox couple potentials shift by 600–800 mV. As a consequence, the diethyl derivative, for example, gives rise to reduced species (19 or 20 VE) which are not observed for **1**. The implications of these results for the reduction of N_2 within the coordination sphere of the FeMo cofactor of nitrogenases are discussed.

Keywords
cyclic voltammetry · iron complexes · redox systems · structure elucidation · sulfur ligands

Introduction

The coupled transfer of protons and electrons is an essential feature of numerous redox reactions catalyzed by reductases. This process involves conversion of the substrate **S** into the product **P** according to Equation (1).[1] An important point

$$S + xH^+ + ye^- \longrightarrow P \qquad (1)$$

concerns the order of these two transfer steps.[1] In particular, if the redox reaction takes place at the active site of a reductase containing an [M_xS_y] aggregate (e.g. as in nitrogenases), the question arises as to whether or not the initial transfer of protons can influence the metal–sulfur core, the small molecules (such as CO or N_2) bound to the core, and the subsequent transfer of electrons.

In order to shed light upon this problem, we have investigated the protonation, alkylation, and redox properties of complexes with the [Fe("N_HS_4")] fragment ("N_HS_4"$^{2-}$ = 2,2′-bis(2-mercaptophenylthio)diethylamine(2 −)). This fragment contains an Fe^{II} center in a sulfur-rich coordination sphere and can exist in the diastereomeric forms **A** and **B**. These two forms can bind either σ–π ligands such as CO or N_2H_2 (form **A**) or σ ligands such as N_2H_4, NH_3, or MeOH (form **B**).[2]

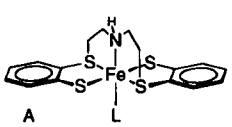

A

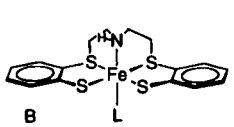

B

[*] Prof. Dr. D. Sellmann, Dr. T. Becker, Dr. F. Knoch
Institut für Anorganische Chemie der Universität Erlangen-Nürnberg
Egerlandstr. 1, D-91058 Erlangen (Germany)
Fax: Int. code +(9131)857-367
e-mail: sellmann@anorganik.chemie.uni-erlangen.de

[**] Transition Metal Complexes with Sulfur Ligands, Part 120. Part 119: D. Sellmann, T. Becker, F. Knoch, *Chem. Ber.* **1996**, *119*, 509–519. "N_HS_4"$^{2-}$ = 2,2′-Bis(2-mercaptophenylthio)diethylamine(2 −).

0947-6539/96/0209-1092 $ 15.00+.25/0

Results

Protonation and alkylation of [Fe(CO)("N_HS_4")] (1): The addition of one equivalent of CF_3SO_3H to a CH_2Cl_2 solution of **1** at −78 °C resulted in a color change from red to red-violet. The CO band at $\tilde{\nu} = 1965\ cm^{-1}$ in the IR spectrum of **1** was replaced by another CO band at $\tilde{\nu} = 1999\ cm^{-1}$, which was assigned to the complex [Fe(CO)("N_HS_4"-H)](CF_3SO_3) (**2**). Addition of a second equivalent of CF_3SO_3H gave an orange solution, and a CO band at $\tilde{\nu} = 2044\ cm^{-1}$ due to the formation of [Fe(CO)("N_HS_4"-H_2)]$(CF_3SO_3)_2$ (**3**) was detected; an SH band at $\tilde{\nu} = 2442\ cm^{-1}$ could also be observed. Subsequent addition of Et_2O or H_2O to the reaction mixture regenerated **1** as determined by IR spectroscopy. These results are consistent with the stepwise and reversible protonation of the thiolato donors in **1** according to Scheme 1. The ν(CO) shifts can be explained by a decrease in electron density at the Fe center leading to a weakening of the Fe–CO π back-bonding.

In order to achieve complete and reversible reactions, it was necessary to work at temperatures below −30 °C. Decomposition of **1** was observed at 0 °C and above, as indicated by the slow decrease in the ν(CO) intensities. Only monoprotonation of **1** could be achieved when an Et_2O solution of HBF_4 (a weaker Brönsted acid than CF_3SO_3H in CH_2Cl_2) was used.

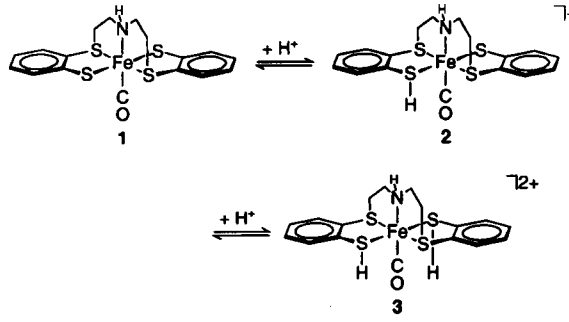

Scheme 1. Stepwise and reversible protonation of the thiolato donors in **1**.

Since all attempts to isolate the thiol complexes **2** and **3** were unsuccessful, we decided to prepare the isoelectronic alkyl derivatives. Alkylation of **1** with one equivalent of Me_3OBF_4 or Et_3OBF_4 gave the monoalkylated complexes **4** and **5**, respectively, in good yields as red microcrystals (step (i), Scheme 2). Both

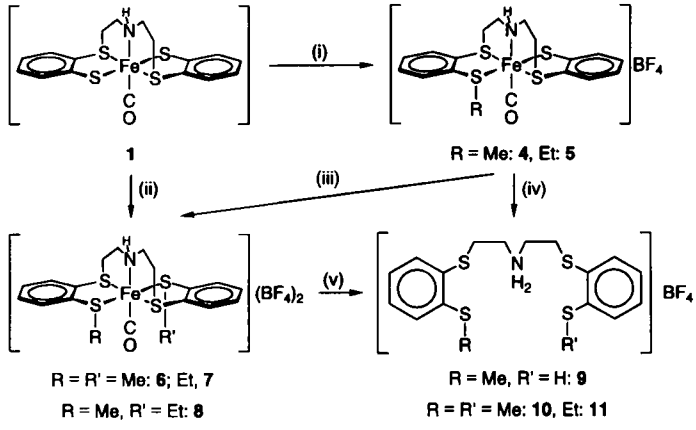

Scheme 2. Alkylation reactions of **1**: i) and iii) Me_3OBF_4 or Et_3OBF_4, 1 equiv; ii) Me_3OBF_4 or Et_3OBF_4, 2 equiv; iv) and v) conc. HCl/MeOH at reflux.

4 and **5** are soluble in CH_2Cl_2, $CHCl_3$, acetone, nitroalkanes, CH_3CN, and MeOH. Treatment of **1** with two equivalents of Me_3OBF_4 or Et_3OBF_4 (step (ii)) yielded the dialkylated derivatives **6** and **7**, respectively. Furthermore, treatment of **1** with one equivalent of Me_3OBF_4 followed by the addition of one equivalent of Et_3OBF_4 gave the "asymmetric" dialkyl derivative **8** (steps (i) + (iii)). The second alkylation always took considerably longer (ca. 15 h) than the first (15 min), a fact explained by the significant decrease in nucleophilicity of the remaining thiolato donor in the monoalkyl derivatives.

Complexes **6**, **7**, and **8** all precipitated from the reaction mixtures as orange powders. Each was obtained in crystalline form by recrystallization from MeOH/Et_2O or $EtNO_2$/Et_2O. Complexes **4**–**8** are soluble in MeOH, MeCN, acetone, and nitroalkanes; complexes **4** and **5** are also soluble in CH_2Cl_2 and $CHCl_3$.

Synthesis and ligation properties of new open-chain thioether amine thiols: Acidic hydrolysis of the alkylated complexes **4**, **6**, and **7** with concentrated hydrochloric acid in refluxing MeOH yielded the free ligands, which were isolated as the ammonium tetrafluoroborate salts **9**, **10**, and **11**, respectively (steps (iv) and (v), Scheme 2). The free ligands **9**–**11** are all soluble in CH_2Cl_2,

Abstract in German: *Welche Effekte ergeben sich bei Protonierungs- und Alkylierungsreaktionen von Schwefeldonoren in Metall-Schwefel-Komplexen? Diese Frage wurde am Beispiel des 18-Valenzelektronen (VE)-Komplexes [Fe(CO)("N_HS_4")] **1**, in dem der fünfzähnige Thioether-Thiolat-Amin-Ligand "N_HS_4"$^{2-}$ (= 2,2'-Bis(2-mercaptophenylthio)diethylamin(2−)) an ein low-spin-Fe^{II}-Zentrum koordiniert ist, untersucht. Die beiden Thiolatdonoren in **1** können reversibel protoniert werden. Die ν(CO)-Frequenz erhöht sich im ersten Protonierungsschritt um 35 cm^{-1} und im zweiten um 45 cm^{-1}. Die Alkylierung von **1** mit einem oder zwei Äquivalenten der Oxoniumsalze R_3OBF_4 (R = Me, Et) führt zu [Fe(CO)("N_HS_4"-R)]BF_4 (R = Me: **4**, Et: **5**), [Fe(CO)("N_HS_4"-R_2)]$(BF_4)_2$ (R = Me: **6**, Et: **7**) und dem Methyl-Ethyl-Derivat [Fe(CO)("N_HS_4"-Me-Et)]$(BF_4)_2$ **8**. Dabei wird für jeden der aufeinanderfolgenden Alkylierungsschritte eine Erhöhung der ν(CO)-Frequenz um 31–32 cm^{-1} beobachtet. Aufgrund der C_1-Symmetrie von **1** bilden sich **4**, **5** und **8** als 1:1-Gemische zweier Diastereomere, während **6** und **7** jeweils nur ein Diastereomer liefern. Die saure Hydrolyse von **4**, **6** und **7** ergibt die entsprechenden Liganden ['$N_{H2}S_4$'-R_n]$(BF_4)_n$ (**9**–**11**; n = 1,2), die als Ammoniumtetrafluoroboratsalze isoliert wurden. Die Molekülstruktur von **8a** wurde röntgenstrukturanalytisch aufgeklärt. Die Röntgenstrukturanalyse zeigt, daß sich die Fe-N- und Fe-S-Abstände durch die Alkylierung der Thiolatdonoren nicht ändern, obwohl der Unterschied der ν(CO)-Frequenzen von **1** und **8** auf eine deutliche Abnahme der Elektronendichte am Fe-Zentrum hinweist. Die Abnahme der Elektronendichte läßt sich plausibel mit der Zunahme des π-Acceptorcharakters der Schwefeldonoren durch Protonierung oder Alkylierung erklären. Die Veränderung der Elektronendichte im [Fe("NS_4")]-Gerüst wird darüber hinaus durch die cyclovoltametrischen Untersuchungen bekräftigt. Das Redoxpotential jedes Redoxpaares wird in jedem Schritt der aufeinanderfolgenden Protonierungen oder Alkylierungen um 600–800 mV verschoben. Als Folge davon treten beispielsweise im Falle des Diethylderivats reduzierte 19 VE- oder 20 VE-Spezies auf, die sich bei **1** nicht beobachten ließen. Die Schlußfolgerungen aus diesen Ergebnissen für die Reduktion von N_2 innerhalb der Koordinationssphäre des FeMo-Cofactors von Nitrogenasen werden diskutiert.*

  0947-6539/96/0209-1093 $ 15.00+.25/0

$CHCl_3$, MeOH, acetone, DMF, and DMSO. These ligands are not accessible by conventional alkylation procedures from the free thioether thiol amine ligand "N_HS_4"-H_2. Furthermore, the isolation of **9** allows the coordination chemistry of this ligand to a Fe^{II} center to be investigated according to Equation (2).

$$Fe(CF_3SO_3)_2 + \text{"}N_HS_4\text{"-Me-Li} \xrightarrow[1,4\text{-dioxane}]{2\text{ h, reflux}} \underset{\mathbf{12}}{[Fe(CF_3SO_3)(\text{"}N_HS_4\text{"-Me})]} \xrightarrow{+\ CO} [Fe(CO)(\text{"}N_HS_4\text{"-Me})](CF_3SO_3) \quad (2)$$

Complex **12** was isolated as a yellow-green powder and is soluble in CH_2Cl_2, $CHCl_3$, THF, dioxane, DMSO, and DMF. It is paramagnetic in the solid state; its effective magnetic moment ($\mu_{eff} = 4.96\ \mu_B$, 298 K) is near the spin-only value ($\mu_{eff} = 4.90\ \mu_B$) expected for a pseudooctahedral high spin Fe^{II} center. Three SO bands at $\tilde{\nu} = 1283, 1239$, and $1028\ cm^{-1}$ can be identified in the IR (KBr) spectrum and indicate that the $CF_3SO_3^-$ anion is coordinated to the Fe center.[3] Addition of CO to complex **12** [Eq. (2)] rapidly gave the cation [Fe(CO)("N_HS_4"-Me)]$^+$, which could be identified by its characteristic CO band at $\tilde{\nu} = 1979\ cm^{-1}$.

Characterization and stereochemistry: The FD mass spectra of the monoalkyl derivatives **4** and **5** reveal peaks for the cations [Fe(CO)("N_HS_4"-Me)]$^+$ and [Fe(CO)("N_HS_4"-Et)]$^+$, respectively. The mass spectra of the dialkyl derivatives only display peaks for the free ligands. Slow decomposition in solution prevented the measurement of $^{13}C\{^1H\}$ NMR spectra of the mono and dialkylated complexes.

The IR (KBr) spectra of the ligand salts **9–11** exhibit broad but characteristic NH_2 bands in the region $\tilde{\nu} = 2725–2675\ cm^{-1}$ as well as a strong BF_4 band at $\tilde{\nu} \approx 1040\ cm^{-1}$. The characteristic CO bands of these complexes serve as a probe for the electron density at the [Fe("NS_4")] core. The ν(CO) frequencies for complexes **1–8** are listed in Table 1; an increase in ν(CO) of 31–32 cm^{-1} is observed for each successive alkylation. This increase parallels the ν(CO) shifts observed when a CH_2Cl_2 solution of **1** (1956 cm^{-1}) is protonated to give **2** (1999 cm^{-1}) and **3** (2044 cm^{-1}). These shifts indicate that both protonation and alkylation take place at the thiolato donors (Scheme 1).

Table 1. IR CO frequencies of complexes **1–8**.

Complex	ν(CO), solution [cm^{-1}]	ν(CO), KBr [cm^{-1}]
[Fe(CO)("N_HS_4")] (**1**)	1965 [a],1957 [b]	1954
[Fe(CO)("N_HS_4"-H)]CF_3SO_3 (**2**)	1999 [a]	
[Fe(CO)("N_HS_4"-Me)](BF_4) (**4**)	1989 [b]	1973
[Fe(CO)("N_HS_4"-Et)](BF_4) (**5**)	1988 [b]	1971
[Fe(CO)("N_HS_4"-H_2)]$(CF_3SO_3)_2$ (**3**)	2044 [a]	1983
[Fe(CO)("N_HS_4"-Me_2)]$(BF_4)_2$ (**6**)	2021 [b]	2023
[Fe(CO)("N_HS_4"-Et_2)]$(BF_4)_2$ (**7**)	2020 [b]	2023
[Fe(CO)("N_HS_4"-Me-Et)]$(BF_4)_2$ (**8**)	2020 [b]	2026

[a] In CH_2Cl_2. [b] In $EtNO_2$.

The SMe and SEt signals in the ^1H NMR spectra were used to determine the stereochemistry of the alkylated derivatives and indicated the formation of diastereomers in the case of **4**, **5**, and **8**: complex **1** possesses C_1 symmetry and consequently exhibits stereochemically inequivalent thiolato S atoms (S(1) and S(4), Fig. 1).[2b] Accordingly, the monoalkylation of **1** yielded a 1:1 mixture of diastereomers of **4** or **5**, resulting from reaction at either the S(1) or S(4) atom. Only one stereoisomer was obtained when the second thiolato donor was alkylated with a second equivalent of the same R_3OBF_4, to give the dialkyl derivatives **6** or **7**. In the case of the "asymmetrical" dialkyl derivative **8**, a 1:1 mixture of diastereomers was obtained.

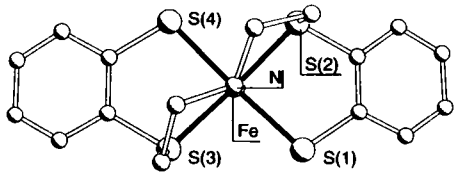

Fig. 1. View along the Fe–N axis of **1**.

X-ray structure analysis of 4 and 8: One of the diastereomers of the monomethyl derivative **4** could be isolated by crystallization and characterized by X-ray structure analysis. The poor quality of the crystals, however, only allowed the confirmation of the atom connectivities as indicated in **4a**. Complexes **4a** and **4b** represent the diastereomers formed by methylation of the S(1) and S(4) thiolato donors of **1**, respectively (Fig. 1).

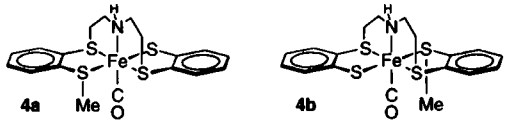

The diastereomeric mixture of **8** could also be separated by crystallization. The molecular structure of one isomer (**8a**) was determined by X-ray structure analysis (Fig. 2). Table 2 compares selected bond lengths and angles of **8a** with those of the parent compound **1**.

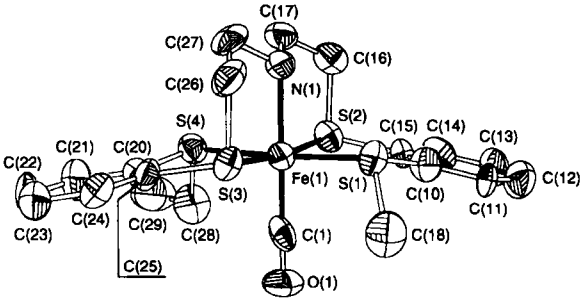

Fig. 2. ORTEP PLOT of the cation of **8a** (drawn with ellipsoids at the 50% probability level; H atoms omitted).

Table 2. Comparison of selected bond lengths [pm] and angles [°] for complexes **8a** and **1**.

Bond	**8a**	**1**	Angle	**8a**	**1**
Fe(1)–C(1)	177.2(12)	175.3(12)	C(1)-Fe(1)-S(2)	94.4(4)	93.6(3)
Fe(1)–N(1)	203.4(9)	207.2(8)	S(1)-Fe(1)-N(1)	87.7(3)	88.7(2)
Fe(1)–S(1)	227.1(4)	229.8(3)	S(1)-Fe(1)-S(2)	88.9(1)	88.7(1)
Fe(1)–S(2)	224.5(4)	222.5(3)	S(2)-Fe(1)-S(4)	92.3(1)	88.9(1)
Fe(1)–S(3)	224.4(4)	225.1(3)	S(2)-Fe(1)-S(3)	172.0(1)	172.4(1)
Fe(1)–S(4)	229.1(4)	230.5(3)	C(1)-Fe(1)-N(1)	179.3(5)	176.4(5)

Complex **8a** consists of discrete [Fe(CO)("N_HS_4"-Me-Et)]$^{2+}$ cations and BF_4^- anions. The Fe center is pseudooctahedrally coordinated by the amine N, the carbon monoxide C, and the four thioether S donors, which occupy identical positions to those in the parent complex **1**. The Fe–C, Fe–N, and Fe–S bond lengths in both **8a** and **1** are characteristic for low-spin

0947-6539/96/0209-1094 $ 15.00+.25/0 Chem. Eur. J. 1996, 2, No. 9

Fe^{II}.[4] Four of the five distances in the [Fe("NS_4")] core appear to decrease and one appears to increase slightly upon alkylation of **1** to give **8a**. These changes, however, are insignificant within the 3σ criterion. This consistency is noteworthy when compared to the large changes observed in the Fe–N and Fe–S distances (18 and 22 pm, respectively) in [Fe(CO)("N_HS_4")] upon substitution of the CO ligand with either N_2H_4, NH_3, or MeOH.[2c] Thus, alkylation of the thiolato donors in **1** does not result in geometrical changes in the [Fe("NS_4")] core despite the considerable electronic changes indicated by the ν(CO) shifts.

Cyclic voltammetry: Alkylation and protonation of **1** produce essentially identical ν(CO) shifts. This observation suggests that both the alkyl groups and the protons are bound to the thiolato donors in **1** and, thus, affect the [Fe("NS_4")] core in an analogous manner. This is further reflected in the electrochemical behavior shown in Figure 3. All potentials quoted in Table 3 and Figure 3 are quoted versus NHE.

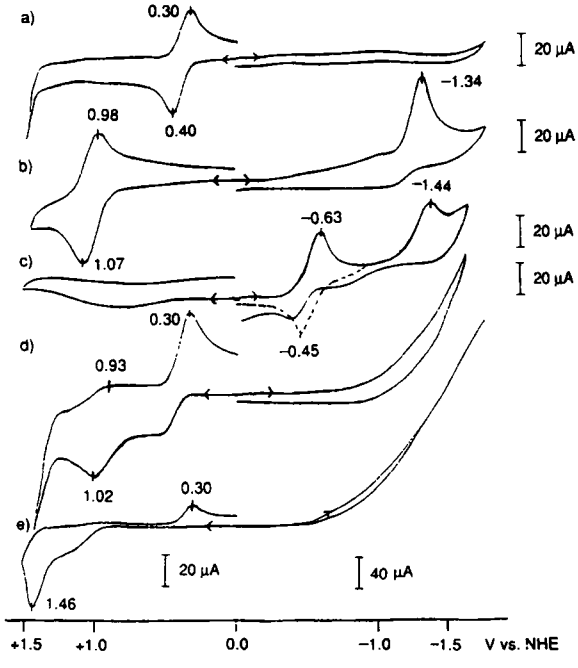

Fig. 3. Cyclic voltammograms of a) **1**, b) ethyl derivative **5**, c) diethyl derivative **7**, d) **1** + 1 CF_3SO_3H, and e) **1** + 2 CF_3SO_3H, in CH_2Cl_2, $c = 10^{-3}$ M, $v = 100$ mV s^{-1}; a–c) recorded at room temperature, d) and e) at −78 °C.

Table 3. Selected electrochemical data for **1**, the mono- and diprotonated derivatives **2** and **3**, and the mono- and dialkylated species **5** and **7**. Supporting electrolyte: NBu_4PF_6 ($c = 0.1$ M).

Complex	E^0 [V] [a]	ΔE_p [V] [b]	I_{pa}/I_{pc}	Redox couples	
1	+0.35 (qr)	0.096	0.84	[Fe(CO)("N_HS_4")]$^{0/+}$	Fe^{II}/Fe^{III}
2	+0.98 (qr)	0.093	0.82	[Fe(CO)("N_HS_4"-H)]$^{+/2+}$	Fe^{II}/Fe^{III}
3	+1.46 (ir)	-	-	[Fe(CO)("N_HS_4"-H_2)]$^{2+/3+}$	Fe^{II}/Fe^{III}
5	+1.02 (qr)	0.123	0.83	[Fe(CO)("N_HS_4"-Et)]$^{+/2+}$	Fe^{II}/Fe^{III}
	−1.34 (ir)	-	-	[Fe(CO)("N_HS_4"-Et)]$^{+/0}$	Fe^{II}/Fe^{I}
7	−0.54 (qr)	0.172	1.13	[Fe(CO)("N_HS_4"-Et_2)]$^{2+/+}$	Fe^{II}/Fe^{I}
	−1.44 (ir)	-	-	[Fe(CO)("N_HS_4"-Et_2)]$^{+/0}$	Fe^{I}/Fe^{0}

[a] vs. NHE, qr = quasireversible, ir = irreversible. [b] $v = 100$ mV s^{-1}.

Complex **1** displays one quasireversible redox wave in the anodic direction at 0.35 V, which can be assigned to the redox pair [Fe(CO)("N_HS_4")]$^{0/+}$ or to an Fe^{II}/Fe^{III} couple. This redox process is solvent dependent, since the wave is shifted to 0.76 V in DMF.[5] The corresponding redox couple of the monoalkyl derivative **5** at 1.02 V is also quasireversible, but is shifted to a higher potential. In contrast to the parent complex, which exhibits no redox wave in the cathodic direction, **5** shows an irreversible redox wave at −1.34 V. This electrochemical process can be assigned to the redox pair [Fe(CO)("N_HS_4"-Et)]$^{+/0}$, which is equivalent to a Fe^{II}/Fe^{I} couple or the reductive formation of the 19 VE species [Fe(CO)("N_HS_4"-Et)]^0. The dialkylated derivative **7** exhibits two waves in the cathodic direction. The quasireversible wave at −0.54 V and the irreversible wave at −1.44 V can be assigned to Fe^{II}/Fe^{I} and Fe^{I}/Fe^{0} couples or the formation of the 19 VE species [Fe(CO)("N_HS_4"-Et_2)]$^+$ and the 20 VE complex [Fe(CO)("N_HS_4"-Et_2)]^0, respectively.

The electrochemical properties of complexes **1**, **5**, and **7** reveal a clear trend in that each alkylation of the thiolato donors increases the potential of the corresponding redox couple by ca. 0.7 V. In other words, the alkylated derivatives become more difficult to oxidize and easier to reduce relative to complex **1**. As a result, the dialkylated derivative **7** can no longer be oxidized, but it can be reduced to give 19 and 20 VE species.

The cyclic voltammograms of CH_2Cl_2 solutions of **1** in the presence of one and two equivalents of CF_3SO_3H are shown in Figures 3d and e, respectively. The different intensities of the oxidation and reduction waves at 0.40 and 0.30 V and at 1.02 and 0.93 V in the anodic direction indicate equilibria between protonated and unprotonated species according to Scheme 1. In the cathodic direction the irreversible reduction of protons to dihydrogen prevents the observation of defined redox waves.

Based on the equilibria shown in Scheme 1, the cyclic voltammogram in Figure 3d reveals the redox couple for the unprotonated [Fe(CO)("N_HS_4")]$^{0/+}$ at 0.35 V as well as a second redox wave at 0.98 V, which can be assigned to the Fe^{II}/Fe^{III} oxidation of the protonated [Fe(CO)("N_HS_4"-H)]$^+$ species. Thus, a comparison of Figures 3b and 3d reveals that both alkylation and protonation lead to an essentially identical increase in the oxidation potential. In the presence of two equivalents of CF_3SO_3H (Fig. 3e), the redox wave at 0.98 V seen in Figure 3d is significantly reduced in intensity, and a new redox wave at 1.46 V appears, which has been tentatively assigned to the oxidation of the doubly protonated species [Fe(CO)("N_HS_4"-H_2)]$^{2+}$.

Discussion

The order and the mutual influence of the proton and electron transfer steps that take place at the active sites of reductases containing metal–sulfur centers have been largely unexplored. The investigation of [Fe(CO)("N_HS_4")] (**1**) was expected to shed some light upon this problem.

Complex **1** contains an Fe^{II} center in a sulfur-rich coordination sphere. The NH and thiolato S donors provide three sites at which Brönsted acid–base reactions can take place. In addition, the CO band in the IR spectrum provides a sensitive probe for studying electronic effects. Sequential protonation of **1** (ν(CO) = 1965 cm^{-1}) by two equivalents of CF_3SO_3H results in an increase in ν(CO) of 34 cm^{-1} after the addition of the first equivalent and 45 cm^{-1} after the second. As previously observed, complex **1** can also be deprotonated by *n*BuLi at the NH functionality to give Li[Fe(CO)("NS_4")] with a ν(CO) frequency lowered by 25 cm^{-1}.[6] Thus complex **1** can exist in four different protonated states. The changes in ν(CO) can be explained by an increase or decrease in electron density at the Fe center leading to a strengthening or weakening of the Fe–CO π backbonding, respectively. The relatively large change in the ν(CO) shift of over 100 cm^{-1} between the deprotonated [Fe(CO)("NS_4")]$^-$ anion and the diprotonated [Fe(CO)("N_HS_4"-

$H_2)]^{2+}$ cation is remarkable. In homoleptic carbonyl complexes, such as $[V(CO)_6]$ (1976 cm^{-1}) and $[V(CO)_6]^-$ (1860 cm^{-1}),[7] such a large $\Delta\nu$(CO) is only observed when the oxidation state of the metal differs by a whole unit. Similar effects (within a more restricted range) have been previously observed for the related complexes $[Fe(CO)_2(\text{"}S_4\text{"})]$, $[Fe(CO)(\text{"}S_5\text{"})]$,[8] [Ru-(CO)("$^{bu}S_5$")],[9] and $[CpFe(CO)_2(SPh)]$.[10]

The protonation and deprotonation of **1** is reversible, and this prevents the isolation of the protonated complexes. In order to confirm the sites of protonation and to obtain fully characterizable species, complex **1** was alkylated yielding the mono alkyl derivatives **4** and **5**, and the dialkyl derivatives **6**, **7**, and **8** (Scheme 2). Hydrolysis of these complexes liberated the free ligands, which are not accessible from "N_HS_4"-H_2 by conventional alkylation methods.

Owing to the C_1 symmetry of **1**, monoalkylation resulted in a 1:1 mixture of two diastereomers, which, upon further alkylation with the same electrophile, gave isomerically pure complexes. The molecular structure of the dialkyl derivative **8a** was elucidated and fully refined by X-ray structure analysis. It shows that, in spite of the different electron densities at the Fe centers in **8a** and **1**, as indicated by the large $\Delta\nu$(CO), the Fe–N and Fe–S bond lengths of **8a** are essentially identical to those of the parent complex **1**. This demonstrates the remarkable electronic flexibility of the [Fe("NS_4")] core, which can be traced back to the bonding characteristics of thioether and thiolato sulfur donors. These sulfur donors can act as σ-donor, σ-donor/π-donor, or σ-donor/π-acceptor ligands.[11] In order to explain the unaltered distances between complexes **1** and **8**, we suggest the bonding scheme shown in Figure 4. The Fe-S(thiolato)

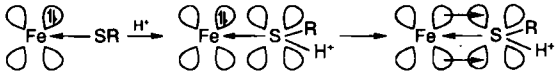

Fig. 4. Suggested bonding scheme for the [Fe("NS_4")] complexes.

bonds are assumed to have predominantly σ-donor bond character. Both alkylation and protonation of the thiolato S donors lead to a weakening of the Fe–S σ bond and an inductive withdrawal of electron density from the Fe center. These thioether or thiol donors, however, gain π-acceptor character such that partial Fe → S π back-donation can occur leading to a further decrease in electron density at the Fe center. The Fe-S distances remain unchanged because the weakening of the S → Fe σ-donor bond is compensated by the formation of the Fe → S π back-bond. A general consequence is that these metal sulfur cores can facilitate the uptake and release of electrons since no additional activation barriers due to the rearrangement of atoms, distances, angles, etc. exist to impede electron transfer.[12] In addition, decreased electron density in the core is expected to favor reduction of these complexes.

Effects similar to those described here were recently observed for the related complexes $[Fe(CO)_2(\text{"}S_4\text{"})]$ and $[Fe(CO)(\text{"}S_5\text{"})]$.[8] However, these complexes display no redox waves between +1.5 and −1.5 V. In contrast, complex **1** and its alkylated and protonated derivatives exhibit well defined redox processes. The cyclic voltammograms show that each step of alkylation, or protonation, shifts the potential of the corresponding redox pairs by about 700 mV. As a consequence, the alkylated or protonated species are more difficult to oxidize and easier to reduce. The 19 or 20 VE complexes, which are not electrochemically observed for the neutral parent complex **1**, are accessible when one or both thiolato donors are alkylated. These results are consistent with our previous discussions that the alkylated derivatives can serve as models for the protonated species.[8, 9, 13]

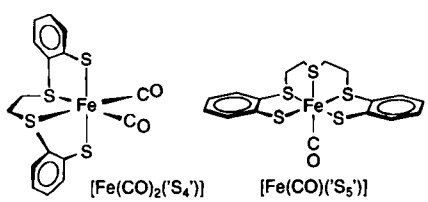

The results reported here may also be significant for biological N_2 fixation.[14] It has been taken for granted that the N_2 molecule binds to the FeMo cofactor of nitrogenases. The structure–function relationship that exists between the Fe–S distances and redox properties of $[Fe(CO)(\text{"}N_HS_4\text{"}\text{-}R_x)]^x$ ($x = 0, +1, +2$, R = alkyl, H) suggests that protonation of the FeMoco may be necessary in order to facilitate the subsequent transfer of electrons at biologically accessible redox potentials.

Experimental Section

General: All reactions were carried out under nitrogen using Schlenk techniques; solvents were dried and distilled before use. As far as possible, reactions were monitored by IR spectroscopy. Spectra were recorded with the following instruments: IR: Perkin Elmer 16 PC FT-IR, solvent bands were compensated for; NMR: Jeol NMR-Spektrometer JNM-EX270; MS: Varian MAT212; magnetic susceptibility: Johnson Matthey susceptibility balance. Cyclic voltammograms were measured with a PAR 264A potentiostat and a standard three-electrode cell. Electrodes used were a glassy carbon ROTEL A working electrode, a Ag/AgCl reference electrode and a Pt wire auxiliary electrode. Potentials were referenced to NHE via Cp_2Fe/Cp_2Fe^+, which was used as an internal standard [$E^\circ(Cp_2Fe/Cp_2Fe^+)$ = 0.400 V vs. NHE] [15]. NBu_4PF_6 (c = 0.1 M) was used as the supporting electrolyte. [Fe(CO)("N_HS_4")] (**1**) [2b] was prepared according to literature methods.

IR spectroscopic monitoring of the reaction of 1 with CF_3SO_3H: CF_3SO_3H (0.068 mL, 0.77 mmol) was added to a red solution of **1** (335 mg, 0.77 mmol) in 10 mL of CH_2Cl_2 (ν(CO) = 1965 cm^{-1}). The solution instantly became red-purple and the ν(CO) band shifted to 1999 cm^{-1}. Addition of a second equivalent of CF_3SO_3H resulted in a color change to orange and a further ν(CO) shift to 2044 cm^{-1}. Finally, addition of H_2O (0.5 mL) led to the regeneration of **1** and the original band at 1965 cm^{-1}.

[Fe(CO)("N_HS_4"-Me)]BF_4 (4): Solid Me_3OBF_4 (815 mg, 5.49 mmol) was added to a red solution of **1** (2.390 g, 5.49 mmol) in CH_2Cl_2 (100 mL). After 30 min, the red mixture was filtered through filter pulp, reduced in volume to 50 mL, layered with Et_2O (50 mL), and stored at −30 °C. The resulting red microcrystals of the isomeric mixture of **4** were isolated after 1 d, washed with Et_2O (50 mL), and dried in vacuo. Yield: 1.8 g (59%). ^1H NMR (CD_3NO_2): δ = 8.10–7.13 (m, 8H; C_6H_4, **4a**, **4b**), 5.85 (m, 1H; N*H*, **4a**), 5.04 (m, 1H; N*H*, **4b**), 4.07–2.61 (m, 8H; C_2H_4, **4a**, **4b**), 3.01 (s, 3H; CH_3, **4a**) 2.95 (s, 3H; CH_3, **4b**); IR (KBr): $\tilde{\nu}$ = 3224 (NH), 1973 (CO), 1083 cm^{-1} (BF); MS (FD; $EtNO_2$): *m/z*: 450 [Fe(CO)("N_HS_4"-Me)]$^+$, 422 [Fe("N_HS_4"-Me)]$^+$; $C_{18}H_{20}FeBF_4NOS_4$ (537.3): calcd. C 40.24, H 3.75, N 2.61, S 23.87; found C 40.19, H 3.88, N 2.62, S 23.60.

4a: Layering a solution of the isomeric mixture of **4** (200 mg) in CH_2Cl_2 (20 mL) with Et_2O (20 mL) and storage at −30 °C yielded crystals of isomerically pure **4a**, which were isolated after 1 d, washed with Et_2O (10 mL), and dried in vacuo. Yield: 80 mg (40%). ^1H NMR (CD_3NO_2): δ = 8.09 (d, 1H; C_6H_4), 8.01 (d, 1H; C_6H_4), 7.78–7.73 (m, 4H; C_6H_4), 7.26 (t, 1H; C_6H_4), 7.13 (t, 1H; C_6H_4), 5.85 (m, 1H; N*H*), 4.07 (m, 1H; C_2H_4), 3.52–3.35 (m, 5H; C_2H_4), 3.01 (s, 3H; CH_3), 2.81 (m, 1H; C_2H_4), 2.62 (m, 1H, C_2H_4).

[Fe(CO)("N_HS_4"-Et)]BF_4 (5): Solid Et_3OBF_4 (500 mg, 2.63 mmol) was added to a red solution of **1** (1.145 g, 2.63 mmol) in CH_2Cl_2 (50 mL) at 0 °C. The mixture was stirred for 30 min at 0 °C, warmed to room temperature, filtered through filter pulp, reduced to one fourth of its volume, layered with Et_2O (15 mL), and stored at −30 °C. The resulting red microcrystals of the isomeric mixture of **5** were isolated after 1 d, washed with Et_2O (20 mL), and dried in vacuo. Yield: 1.2 g (83%). ^1H NMR (CD_3NO_2): δ = 8.12–7.14 (m, 8H; C_6H_4), 4.99 (t, 1H; N*H*), 4.22 (m, 1H; C_2H_4), 3.44–2.29 (m, 11H; C_2H_4 and CH_2CH_3), 1.63 (m, 3H; CH_2CH_3); IR (KBr): $\tilde{\nu}$ = 3211 (NH), 1971 (CO), 1083 cm^{-1} (BF); MS (FD, CH_2Cl_2): *m/z*: 436 [Fe("N_HS_4"-Et)]$^+$; $C_{19}H_{22}FeBF_4NOS_4$ (551.3): calcd. C 41.39, H 4.02, N 2.54, S 23.27; found C 41.66, H 4.14, N 2.54, S 23.33.

0947-6539/96/0209-1096 $ 15.00+.25/0 Chem. Eur. J. 1996, 2, No. 9

[Fe(CO)("N_HS_4"-R_2)]$(BF_4)_2$ (R = Me: **6**, R = Et: **7**): 4 mmol of R_3OBF_4 (R = Me: 590 mg, R = Et: 800 mg) were added to a red solution of **1** (870 mg, 2 mmol) in CH_2Cl_2 (50 mL). After 15 h, the resulting orange precipitate was removed by filtration and dissolved in MeOH (25 mL). Layering this solution with Et_2O (25 mL) gave an orange microcrystalline material, which was isolated after 1 d, washed with Et_2O (20 mL), and dried in vacuo.

6: Yield: 705 mg (55%). ^{1}H NMR (CD_3NO_2): δ = 8.33–7.75 (m, 8H; C_6H_4), 5.80 (s, 1H; N*H*), 3.76–2.65 (m, 8H; C_2H_4), 3.16 (s, 3H; CH_3), 3.15 (s, 3H; CH_3); IR ($EtNO_2$): $\tilde{\nu}$ = 2021 cm^{-1} (CO); MS (FD, $EtNO_2$): *m/z*: 381 ["N_HS_4"-Me_2]$^+$, 219 [Fe("N_HS_4"-Me_2)]$^{2+}$, 191 ["N_HS_4"-Me_2]$^{2+}$; $C_{19}H_{23}B_2F_8FeNOS_4$ (639.1): calcd. C 35.71, H 3.63, N 2.19, S 20.07; found: C 35.93, H 3.63, N 2.23, S 20.13.

7: Yield: 1.0 g (75%). ^{1}H NMR (CD_3NO_2): δ = 8.28–7.25 (m, 8H; C_6H_4), 5.71 (s, 1H; N*H*), 3.68–2.54 (m, 12H; C_2H_4 and CH_2CH_3); 1.79 (m, 3H; CH_2CH_3); IR (KBr) : $\tilde{\nu}$ = 3207 (NH), 2023 (CO), 1062 cm^{-1} (BF); MS (FD, $EtNO_2$): *m/z*: 409 ["N_HS_4"-Et_2]$^+$, 205 ["N_HS_4"-Et_2]$^{2+}$; $C_{21}H_{27}B_2F_8FeNOS_4$ (667.2): calcd. C 37.80, H 4.08, N 2.10, S 19.23; found C 37.93, H 4.30, N 2.09, S 19.09.

[Fe(CO)("N_HS_4"-Me-Et)]$(BF_4)_2$ (8): Solid Me_3OBF_4 (405 mg, 2.73 mmol) was added to a red solution of **1** (1.19 g, 2.73 mmol) in CH_2Cl_2 (40 mL). After 15 min, Et_3OBF_4 (520 mg, 2.73 mmol) was added to the red-violet solution. After another 15 h, the resulting orange precipitate was filtered off, washed with CH_2Cl_2 (20 mL), and dried in vacuo. Yield: 1.2 g (68%). ^{1}H NMR (CD_3NO_2): δ = 8.24–7.23 (m, 8H; C_6H_4, **8a**, **8b**), 5.78 (m, 1H; N*H*, **8b**), 5.53 (m, 1H; N*H*, **8a**), 3.78–2.51 (m, 10H; C_2H_4 and CH_2CH_3, **8a**, **8b**), 3.16 (s, 3H; CH_3, **8b**), 3.14 (s, 3H; CH_3, **8a**), 1.78 (t, 3H; CH_2CH_3, **8b**), 1.76 (t, 3H; CH_2CH_3, **8a**); IR (KBr): $\tilde{\nu}$ = 3213 (NH), 2026 (CO), 1068 cm^{-1} (BF); MS (FD, $EtNO_2$): *m/z*: 395 ["N_HS_4"-Me-Et]$^+$; $C_{20}H_{25}B_2F_8FeNOS_4$ (653.2): calcd. C 36.78, H 3.86, N 2.14, S 19.64; found C 37.81, H 3.88, N 2.17, S 19.69.

Layering a solution of the isomeric mixture of **8** (200 mg) in $EtNO_2$ (20 mL) with Et_2O (20 mL) yielded single crystals of isomerically pure **8a**. These crystals were isolated after 1 d, washed with Et_2O (10 mL), and dried in vacuo. Yield: 70 mg **8a** (35%). ^{1}H NMR (CD_3NO_2): δ = 8.24–7.71 (m, 8H; C_6H_4), 5.53 (m, 1H; N*H*), 3.72–2.51 (m, 10H; C_2H_4 and CH_2CH_3), 3.14 (s, 3H; CH_3), 1.76 (t, 3H; CH_2CH_3).

["N_HS_4"-R-R']·HBF_4 (R = H, R' = Me: **9**; R = R' = Me: **10**; R = R' = Et: **11**): Conc. hydrochloric acid (0.5 mL, 60 mmol) was added to a red solution of **4** (540 mg, 1 mmol) or an orange solution of [Fe(CO)("N_HS_4"-R_2)]$(BF_4)_2$ (1 mmol; R = Me, **6**: 640 mg; R = Et, **7**: 670 mg) in MeOH (30 mL). The reaction mixture was heated under reflux for 2 h yielding in all cases a light yellow solution. After removal of the solvent, the residue was extracted with CH_2Cl_2 (30 mL), dried with Na_2SO_4 (3 g), and filtered. The solvent was removed and the residue redissolved in CH_2Cl_2 (2 mL). In each case, layering this solution with cyclohexane (5 mL) yielded either a colorless or a light yellow powder of the ammonium tetrafluoroborate salt of the ligand, which was isolated and washed with cyclohexane (5 mL).

["N_HS_4"-H-Me]·HBF_4 (9): Yield: 350 mg (77%). ^{1}H NMR ($CDCl_3$): δ = 8.90 (s, 2H; NH_2), 7.52–7.17 (m, 8H; C_6H_4), 4.13 (s, 1H; S*H*), 3.32–3.17 (m, 4H; C_2H_4), 2.44 (s, 3H; CH_3); IR (CH_2Cl_2): $\tilde{\nu}$ = 2702 (NH), 2577 cm^{-1} (SH); MS (FD, CH_2Cl_2): *m/z*: 368 ["N_HS_4"-H_2-Me]$^+$; $C_{17}H_{22}BF_4NS_4$ (455.5): calcd. C 44.83, H 4.87, N 3.08; found C 45.72, H 4.95, N 2.37.

["N_HS_4"-Me_2]·HBF_4 (10): Yield: 360 mg (77%). ^{1}H NMR ($CDCl_3$): δ = 8.68 (br, 2H; NH_2), 7.54–7.19 (m, 8H; C_6H_4), 3.70–2.90 (m, 8H; C_2H_4), 2.46 (s, 6H; CH_3); ^{13}C{^{1}H} NMR ($CDCl_3$): δ = 143.0, 134.3, 129.8, 129.6, 126.1, 125.5 (C_6H_4), 48.7, 32.3 (C_2H_4), 16.4 (CH_3). IR (KBr): $\tilde{\nu}$ = 2744 (NH), 1032 cm^{-1} (BF); MS (FD, CH_2Cl_2): *m/z*: 381 ["N_HS_4"-Me_2]$^+$; $C_{18}H_{24}ClNS_4$ (469.5): calcd. C 46.05, H 5.15, N 2.98; found: C 45.84, H 5.11, N 2.95.

["N_HS_4"-Et_2]·HBF_4 (11): Yield: 370 mg (74%). ^{1}H NMR (CD_2Cl_2): δ = 8.88 (s, 2H; NH_2), 7.50–7.15 (m, 8H; C_6H_4), 3.35–2.94 (m, 12H; C_2H_4 and CH_2CH_3), 1.32 (t, 3H; CH_2CH_3); ^{13}C{^{1}H} NMR (CD_2Cl_2): δ = 140.7, 133.1, 131.8, 129.0, 127.9, 126.7 (C_6H_4), 47.3, 31.0 (C_2H_4), 27.3 (CH_2(Et)), 14.0 (CH_3(Et); IR (KBr): $\tilde{\nu}$ = 2675 (NH), 1041 cm^{-1} (BF); MS (FD, acetone): *m/z*: 410 ["N_HS_4"-Et_2-H]$^+$; $C_{20}H_{28}ClNS_4$ (497.5): calcd. C 48.28, H 5.67, N 2.82, found C 48.52, H 5.93, N 2.31.

[Fe(CF_3SO_3)("N_HS_4"-Me)] (12): A solution of $AgCF_3SO_3$ (255 mg, 1 mmol) in MeOH (10 mL) was added dropwise to a solution of $FeCl_2·4H_2O$ (100 mg, 0.5 mmol) in MeOH (10 mL). The white precipitate of AgCl was removed by filtration after 15 min. Removal of the solvent in vacuo yielded 335 mg (0.5 mmol) of $Fe(CF_3SO_3)_2$.

LiOMe (1 mmol, 1 mL of a 1 M solution in MeOH) was added to a solution of **9** (230 mg, 0.5 mmol) in MeOH (15 mL). The solvent was removed in vacuo and the residue was dissolved in 1,4-dioxane (10 mL). In order to remove LiCl, the resulting suspension was filtered through filter pulp. The filtrate was combined with a solution of $Fe(CF_3SO_3)_2$ (355 mg, 0.5 mmol) (see above) in 1,4-dioxane (10 mL) and heated under reflux for 2 h. The solvent of the green-brown reaction mixture was removed in vacuo, and the resulting residue was dissolved in CH_2Cl_2 (10 mL). Layering this solution with Et_2O led to precipitation of yellow-green microcrystals. These crystals were isolated by filtration, washed with Et_2O (10 mL), and dried in vacuo. Yield: 195 mg (68%). IR (KBr): $\tilde{\nu}$ = 1283, 1239, 1028 cm^{-1} (SO); MS (EI, 70 eV): *m/z*: 571 [Fe(CF_3SO_3)("N_HS_4"-Me)]$^+$, 422 [Fe(CF_3SO_3)("N_HS_4"-Me)]; MS (FD, THF): *m/z*: 571 [Fe(CF_3SO_3)("N_HS_4"-Me)]$^+$, 422 [Fe("N_HS_4"-Me)]; $C_{18}H_{20}F_3FeNO_3S_5$ (571.6): calcd. C 37.83, H 3.53, N 2.45, S 28.05; found C 37.66, H 3.83, N 2.46, S 27.35.

X-ray structure analysis of 8a: Orange needles of **8a** were obtained by layering a saturated $EtNO_2$ solution of the diastereomeric mixture of **8** with Et_2O. A suitable single crystal was sealed in a glass capillary. Intensity data and lattice parameters were measured on a Siemens P4 diffractometer with $Mo_{K\alpha}$ radiation (graphite-monochromator, λ = 71.073 pm). Intensity data were corrected for Lorentzian polarization in the usual manner; absorption corrections were not applied. The structure was solved by direct methods using the SHELXTL-PLUS program package [16]. The function minimized during full-matrix least-squares refinement was $\sum w(|F_o| - |F_c|)^2$. The nonhydrogen atoms were refined using anisotropic thermal parameters; the hydrogen atoms were refined using common isotropic temperature factors. The positions of the hydrogen atoms were taken from the difference Fourier synthesis and restricted during refinement. Further details of the crystal structure investigation may be obtained from the Fachinformationszentrum Karlsruhe, 76344 Eggenstein-Leopoldshafen (Germany) on quoting the depository number CSD-404295. Selected crystallographic data are listed in Table 4.

Table 4. Selected crystallographic data for [Fe(CO)("N_HS_4"-Me-Et)]$(BF_4)_2$ (**8a**).

formula	$C_{20}H_{25}B_2F_8FeNOS_4$
M_r [g mol^{-1}]	653.1
crystal size [mm^3]	0.7 × 0.2 × 0.2
crystal system	monoclinic
space group	$P2_1/c$
a (pm)	1137.8(5)
b (pm)	1418.8(7)
c (pm)	1734.5(6)
β (°)	105.66(3)
V (pm^3)	2696(2) × 10^6
Z	4
ρ_{calcd} (g cm^{-3})	1.609
$\mu_{MoK\alpha}$ (cm^{-1})	9.41
T (K)	293
scan technique	ω-scan
2θ range (°)	3–54
scan speed (° min^{-1})	3–29.3
reflections measured	7787
independent reflections	5887
observed reflections	1968
σ-criterion	$F > 4\sigma(F)$
refined parameters	334
R [a]	0.059
R_w [b]	0.052
largest differnce peak (e pm^{-3})	0.67 × 10^{-6}
largest differnce hole (e pm^{-3})	−0.42 × 10^{-6}

[a] $R = \sum||F_o| - |F_c||/\sum|F_o|$; [b] $R_w = \sum[w(|F_o| - |F_c|)]/\sum[w|F_o|]$; $w^{-1} = \sigma^2(F)$.

Acknowledgements: We thank the Deutsche Forschungsgemeinschaft and the Fonds der Chemischen Industrie for financial support as well as S. Emig and Dr. M. Moll for assistance with NMR measurements.

Received: February 2, 1996

[1] K. K. Kramarz, J. R. Norton, *Progr. Inorg. Chem.* **1994**, *42*, 1–65.
[2] a) D. Sellmann, W. Soglowek, F. Knoch, M. Moll, *Angew. Chem.* **1989**, *101*, 1244–1245; *Angew. Chem. Int. Ed. Engl.* **1989**, *28*, 1271–1272; b) D. Sellmann, H. Kunstmann, F. Knoch, M. Moll, *Inorg. Chem.* **1988**, *27*, 4183–4190; c) D. Sellmann, W. Soglowek, F. Knoch, G. Ritter, J. Dengler, *ibid.* **1992**, *31*, 3711–3717.
[3] M. Appel, K. Schloter, J. Heidrich, W. Beck, *J. Organomet. Chem.* **1987**, *322*, 77–88.
[4] a) L. Christiansen, D. N. Hendrickson, H. Toftlund, S. R. Wilson, C. L. Xie, *Inorg. Chem.* **1986**, *25*, 2813–2818; b) J. K. McCusker, H. Toftlund, A. L. Rheingold, D. N. Hendrickson, *J. Am. Chem. Soc.* **1993**, *115*, 1797–1804; c) M. R. Snow, J. A. Ibers *Inorg. Chem.* **1973**, *12*, 249–254; d) D. Sellmann, G. Binker, M. Moll, E. Herdtweck, *J. Organomet. Chem.* **1987**, *327*, 403–418; e) D. Sellmann, R. Weiß, F. Knoch, G. Ritter, J. Dengler, *Inorg. Chem.* **1990**, *29*, 4107–4114.
[5] W. Soglowek, Thesis, Universität Erlangen-Nürnberg, **1992**.
[6] D. Sellmann, T. Hofmann, *Inorg. Chim. Acta* **1994**, *224*, 61–71.
[7] C. Elschenbroich, A. Salzer, *Organometallchemie*, 2nd Ed., Teubner, Stuttgart, **1988**, pp. 269, 277.
[8] D. Sellmann, G. Mahr, M. Moll, F. Knoch, *Inorg. Chim. Acta* **1994**, *224*, 45–59.

  0947-6539/96/0209-1097 $ 15.00+.25/0

[9] D. Sellmann, C. Rohm, M. Moll, *Z. Naturforsch. Teil B* **1995**, *50b*, 1729–1738.
[10] P. M. Treichel, L. D. Rosenhein, *Inorg. Chem.* **1981**, *20*, 942–944.
[11] D. Sellmann, M. Geck, F. Knoch, G. Ritter, J. Dengler, *J. Am. Chem. Soc.* **1991**, *113*, 3819–3828.
[12] a) F. Basolo, R. G. Pearson, *Mechanismen in der anorganischen Chemie*, Thieme, Stuttgart, **1973**, Chapt. 6; b) D. Katakis, G. Gordan, *Mechanisms of Inorganic Reactions*, J. Wiley & Sons, New York, **1987**, Chapt. 7.
[13] D. Sellmann, B. Hadawi, F. Knoch, *Inorg. Chim. Acta* **1996**, *244*, 213–220.
[14] M. C. Zerner, K. K. Stavrev, *Chem. Eur. J.* **1996**, *2*, 83–87.
[15] a) R. R. Gagné, C. A. Koval, G. C. Lisensky, *Inorg. Chem.* **1980**, *19*, 2854–2855; b) H. M. Koepp, H. Wendt, H. Strehlow, *Z. Elektrochem.* **1960**, *64*, 483–491.
[16] *SHELXTL-PLUS for Siemens Crystallographic Research Systems*, Release 421/V, Copyright **1990** by Siemens Analytical X-Ray Instruments Inc., Madison; WI.

0947-6539/96/0209-1098 $ 15.00+.25/0